10.2478/v10063-008-0026-3

ANNALES
UNIVERSITATIS MARIAE CURIE-SKŁODOWSKA
LUBLIN – POLONIA

VOL. LXIII, 3 SECTIO AA 2008

On the stability of magnetic colloids♣

M. T. López-López, G. R. Iglesias, J. D. G. Durán, F. González-Caballero[1]
Department of Applied Physics, Faculty of Sciences,
University of Granada, c/Campus de Fuentenueva s/n 18071 Granada. Spain
[1]*Maria Curie-Skłodowska University, Lublin, Poland*

In this paper, the preparation of fluids belonging to ferrofluid (FF) and magnetorheological (MR) categories is described. Furthermore, the effect of different stabilizing additives (thixotropic agents, surfactants, magnetic nanoparticles) and carrier liquids on the sedimentation of these fluids is analyzed. These studies are conducted using: (i) optical and electromagnetic induction techniques for monitoring the stability of dilute and concentrated suspensions, respectively; (ii) contact angle and pendant drop measurements to explain the observed stability in different carriers. The results of these experiments are analyzed in detail and magnetic fluids with improved stability properties are prepared accordingly.

1. INTRODUCTION

Magnetic colloids are a group of materials that exhibit the remarkable property of changing their flow properties under the application of an external magnetic field [1]. They can be classified into: (*i*) ferrofluids (FF), which are stable colloidal dispersions of ferro- or ferrimagnetic nanoparticles in a carrier liquid [2]; and (*ii*) magnetorheological (MR) fluids, which are dispersions of micron-sized magnetic particles [3]. Nano-sized particles (diameter ≈ 10 nm) used in FF are magnetically single-domain and, therefore, they possess a permanent magnetic dipole moment. Because of the existence of magnetic interactions between these particles in the presence of an external magnetic field, the structures formed in these fluids can largely affect their flow behavior. However, even under the application of high magnetic fields, FF manifest only a

♣ Paper dedicated to Professor Emil Chibowski on the occasion of his 65th birthday

relatively modest magnetoviscous response and do not develop a yield stress [1, 4, 5]. On the contrary, micron-sized ferro- or ferrimagnetic particles are magnetically multidomain and attain large magnetic moments under the application of rather weak magnetic fields. As a consequence, MR fluids manifest a high magneto-viscous response characterized by a high yield stress [6, 7]. Due to these properties, MR fluids are field-responsive materials with a broad range of technological applications.

In order to prevent particle aggregation in FF based on non-polar liquids due to van der Waals attraction, and the subsequent gravitational settling, it is necessary to coat the particles with long-chain molecular species (e.g. fatty acids) [4]. In this paper, a series of organic carriers, with increasing dielectric constants, are tested to determine the adequate coupling between the hydrocarbon tail and the carrier molecules that produce stable ferrofluids.

MR fluids are typically formulated using high density materials such as iron, iron alloys or metal oxides (ceramic ferrites) dispersed in low-density liquids. Therefore, their stabilization against sedimentation arises as an important challenge, facing the technological applications of these field-responsive materials [8]. Approaches to improve the stability include: (*i*) addition of thixotropic agents (e.g. carbon fibers and silica nanoparticles) [6, 9]; (*ii*) addition of surfactants (e.g. oleic acid or stearate salts) [10, 11]; (*iii*) mixing magnetic nanoparticles [12, 13]; and (*iv*) use of viscoplastic media or water-in-oil emulsions as continuous phases [14, 15]. In this paper, we report on the possibility of stabilizing iron-MR fluids using different surfactants (oleic acid, aluminum stearate) as well as using thixotropic agents (silica nanoparticles). In addition, we describe the preparation of magnetic fluid composites (MFC) by dispersing micron-sized iron particles in ferrofluids and we analyze their stability properties. Due to the opaqueness of the MR fluids and MFC studied, the use of classical optical methods is not always suitable to characterize the sedimentation behavior of these systems. Therefore, we have also used an electromagnetic method to measure the sedimentation rate in these suspensions [16]. Using this method, the effect of the surfactant or silica concentration (in MR fluids) and of the nano-magnetite volume fraction (in MFC) on the stability of the suspensions is analyzed and discussed.

2. FERROFLUIDS

2.1. Ferrofluid Preparation and Particle Morphology

The ferrofluids consisted of magnetite nanoparticles covered by oleate molecules dispersed in different organic media. The magnetite particles are synthesized by coprecipitation of Fe(II) and Fe(III) salts in aqueous solutions, and the surfactant used to stabilize the suspensions was oleic acid. This fatty

acid imposes a steric barrier between the oleate-covered magnetite particles that overcomes the van der Waals and magnetic attractions, avoiding particle aggregation in non-polar carriers.

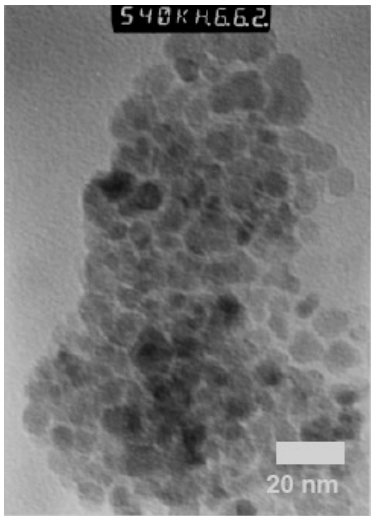

Fig. 1. TEM picture of the magnetite nanoparticles remaining in suspension after centrifugation at 12000×*g*. Liquid carrier: dodecane. Bar length 20 nm. (From [17])

Figure 1 shows a TEM picture of the particles. The average particle diameter after centrifugation at 12000×*g* is shown in Table 1. The particle diameter in the dichloromethane ferrofluid is significantly smaller than in the other carriers. In this ferrofluid a clear gravitational settling is observed as a consequence of particle coagulation, leading to rather diluted suspensions in which only tiny particles remained. The dielectric constants of the liquids used in this work, measured with a Dekameter DK 300 apparatus (WTW Germany), are: 1.8 (mineral oil), 1.8 (kerosene), 2.0 (dodecane), 2.2 (carbon tetrachloride), 4.8 (chloroform), and 9.1 (dichloromethane).

The bulk crystal structure of the synthesized nanoparticles was analyzed by X-ray diffraction and the data showed excellent coincidence with the reference lines for magnetite.

2.2. Interfacial Free Energy of Interaction and Stability

The interfacial free energy of interaction between oleate-covered magnetite nanoparticles immersed in the different carriers was calculated from previous estimation of the surface free energy of the solid material and the surface tension of the liquid media, following the van Oss' approach [18]. With this aim contact

angle and pendant drop measurements were performed. The results are summarized in Tables 1 and 2.

Tab. 1. Surface free energy components (mJ/m^2) of magnetite nanoparticles, and surface tension components (mJ/m^2) of the carrier liquids at 20.0 ± 0.1 ºC. γ^{LW}: van der Waals component, γ^+: electron-acceptor parameter; γ^-: electron-donor parameter. Last column: average diameter (nm) (D_{TEM}), obtained from TEM pictures, of particles dispersed in the indicated carrier liquids after centrifugation at 12000×g. (From [17]).

	Material	γ^{LW}	γ^+	γ^-	D_{TEM}
SOLID	Oleate-covered magnetite	25.3 ± 0.6	0.15 ± 0.22	5.2 ± 0.3	- - -
	Magnetite	49.3 ± 0.2	0.17 ± 0.01	55.4 ± 0.3	- - -
CARRIER	Kerosene	25	0	0	7.8 ± 0.3
	Mineral oil	24 ± 3	0	0	7.15 ± 0.25
	Dodecane	25.35	0	0	7.9 ± 0.3
	CCl_4	27.0	0	0	6.8 ± 0.3
	Chloroform	27.15	0	0	7.8 ± 0.3
	CH_2Cl_2	53 ± 8	0	0	5.14 ± 0.14
	Water	21.8	25.5	25.5	- - -

Tab. 2. Total free energy of interaction, ΔG_{SLS}^{TOT}, between oleate-covered magnetite nanoparticles in the indicated carriers, and the corresponding Lifshitz-van der Waals and acid-base contributions (ΔG_{SLS}^{LW} ; ΔG_{SLS}^{AB}). All quantities in mJ/m^2. (From [17]).

Carrier	ΔG_{SLS}^{LW}	ΔG_{SLS}^{AB}	ΔG_{SLS}^{TOT}
Kerosene	- 0.002 ± 0.007	- 4 ± 3	- 4 ± 3
Mineral oil	- 0.05 ± 0.04	- 4 ± 3	- 4 ± 3
Dodecane	- 0.0001 ± 0.001	- 4 ± 3	- 4 ± 3
CCl_4	- 0.06 ± 0.04	- 1 ± 5	- 1 ± 5
Chloroform	- 0.05 ± 0.04	- 4 ± 3	- 4 ± 3
Dichloromethane	- 9.3 ± 0.5	- 4 ± 3	- 13 ± 3
Water	- 0.26 ± 0.09	- 52 ± 10	- 52 ± 10

This thermodynamic analysis demonstrates that the observed stability of the suspensions in liquids with $\varepsilon_r < 5$ is well correlated with the very low lyophobic (or acid-base) attraction between the particles, which can be easily surmounted by thermal agitation, since the van der Waals attraction is negligible. On the contrary, for liquids with $\varepsilon_r > 9$, the suspensions become unstable because of the combined action of the van der Waals and lyophobic attractions, the latter being dominant for very polar solvents.

2.3. Magnetic Properties of the Particles and the Ferrofluids

The magnetization, M, of the solid powder and the ferrofluids was measured at 20 ºC as a function of the magnetic field strength, H. Figure 2 shows these curves.

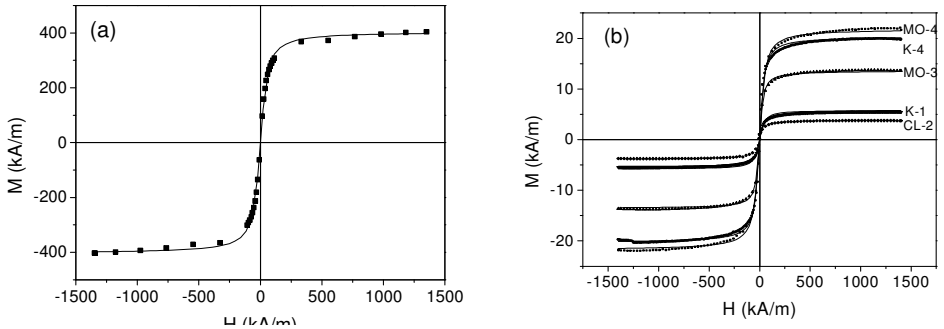

Fig. 2. Magnetization data of: (a) the synthesized oleate-magnetite nanoparticles (powder); (b) the indicated ferrofluids (see sample identification in Table 3). The lines correspond to the best fit to the Langevin function (Equation 2). (From [17]).

The saturation magnetization of the dry powder is $M_s = 4.05 \times 10^5$ A/m and its initial magnetic susceptibility $\chi_i = 5.7$. In addition, the synthesized magnetite has negligible coercivity and remanence, as expected for a superparamagnetic material above the blocking temperature. From these values, the magnetic particle diameter, D_m, can be determined by means of [19]:

$$D_m = \left(\frac{18kT}{\pi\mu_0} \frac{\chi_i}{M_s^2} \right)^{1/3} \tag{1}$$

where k is the Boltzmann constant, T the absolute temperature, and μ_0 the magnetic permeability of vacuum. The calculated magnetic diameter (D_m = 7.60 ± 0.03 nm) is slightly smaller than that estimated from TEM pictures (D_{TEM} = 7.8 nm for ferrofluid in kerosene). The difference between D_m and D_{TEM} can be attributed to the presence of a magnetically "dead" layer on the particle surface, as frequently assumed in the literature [20]. The magnetic moment of each particle, m, can be obtained using the Langevin function [21]:

$$M = M_s \left(\coth \xi - \frac{1}{\xi} \right) \qquad \xi = \frac{\mu_0 m H}{kT} \tag{2}$$

Fitting this function to the magnetization data in Figure 2a, we obtain a magnetic moment $m = (1.38 \pm 0.03)\times10^{-19}$ A·m^2 = $(14900 \pm 300)\mu_B$ per particle, where μ_B is the Bohr magneton.

The saturation magnetization and the initial magnetic susceptibility of the ferrofluids are included in Table 3. The magnetic diameter and the magnetic moment of the particles in the different ferrofluids were determined in a similar way to that followed for dry particles using Equations 1 and 2. The data in Table 3 show that D_m and m for particles immersed in the ferrofluids are slightly larger than those obtained in the dry powder. The significant difference in the magnetic properties (D_m, m) in solid state and in suspension can be attributed to a weak structuration favored by the combined action of both interfacial and magnetic attractions between the particles immersed in the carrier liquid.

Tab. 3. Saturation magnetization (M_s) and initial magnetic susceptibility (χ_i) of the indicated ferrofluid samples (carrier / magnetite volume fraction ϕ). The magnetic diameter (D_m) and magnetic moment (m) of the particles in the ferrofluids were obtained by fitting the magnetization data in Figure 2b to Equations 1 and 2. (From [17]).

Sample Carrier/ϕ (%)	M_s (A/m)	$\chi_i \times 10^3$	D_m (nm)	m (10^{-19} A·m^2)
K-1 Kerosene/ 1.1 ± 0.1	5520 ± 140	337.43 ± 0.12	13.5 ± 0.4	2.02 ± 0.05
K-4 Kerosene/ 4.2 ± 0.1	20400 ± 500	401.07 ± 0.25	9.12 ± 0.07	1.697 ± 0.024
MO-3 Mineral oil/ 2.8 ± 0.1	13800 ± 300	306.33 ± 0.19	9.55 ± 0.11	2.19 ± 0.06
MO-4 Mineral oil/ 4.5 ± 0.1	22000 ± 600	360.53 ± 0.09	8.60 ± 0.06	1.48 ± 0.05
CL-2 Chloroform/ 1.2 ± 0.1	5740 ± 140	260.7 ± 0.3	12.0 ± 0.3	1.68 ± 0.03

3. STABILITY OF MAGNETORHEOLOGICAL FLUIDS

3.1. Sedimentation Behavior in Diluted Suspensions

A. Experimental. Iron powder of HQ quality (BASF, Germany) was used without further treatment. The iron particles are spherical and polydisperse (average diameter 930 ± 330 nm). Silicone oil of viscosity 35.1 ± 0.3 mPa·s and density 954 kg·m^{-3} (Fluka, Germany) and mineral oil of viscosity 39.58 ± 0.16 mPa.s and density 854 kg.m^{-3}, both supplied by Fluka (Germany), were used as liquid carriers. Oleic acid (purity 90%) (Sigma-Aldrich, Germany), and silica

nanoparticles 7 nm in diameter (Aerosil-300®, Degussa-Hüls, Germany) were used as stabilizing additives.

Iron-silica suspensions were prepared as follows: (1) iron, silica and silicone oil were mixed in a polyethylene container; (2) the mixture was shaken and then introduced in a sonifier (Branson model 450, USA). The preparation of iron-OA suspensions involved the following steps: (1) different oleic acid-mineral oil solutions were prepared; (2) iron was added to the selected oil solution; (3) the suspensions were shaken and sonified (Branson model 450, USA); and (4) the samples were stirred (50 rpm; 24 h; 25 ºC) to allow the adsorption of the additive. No significant changes in the viscosity of the carrier were observed as silica nanoparticles or oleic acid content increased in the concentration range employed.

The sedimentation behavior of the suspensions was inferred from the evolution of the optical absorbance of the suspensions. With this aim, a Spectronic 601 spectrophotometer (Milton Roy, USA) at 590 nm of wavelength was used. All studied suspensions contained 1.25 g/L of iron (volume fraction = 0.017%). Samples were placed in square cuvettes with 1 cm of light path. Those were placed in such a way that the center of the light beam struck 1.5 cm above their bottom.

B. Effect of oleic acid. In Figure 3 the normalized optical absorbance, $A_n = A/A_0$ (A_0 is the initial absorbance) is plotted as a function of time for suspensions containing 0.017 vol% of iron and different concentrations of oleic acid (OA). Due to the high density and size of the particles, A_n shows a clear tendency to decrease with time, as a consequence of the progressive disappearance of the iron particles from the lighted region as sedimentation proceeds. The experiments for OA concentration below 16 mM (concentration high enough to complete the first OA adsorbed monolayer, see [22]) show that there is no significant change in the stability of the suspensions for this concentration range. Therefore, it seems that steric repulsion does not play any important role on the sedimentation behavior of iron suspensions at low OA concentration (< 16 mM). However, at high OA concentration (≥ 31 mM) there is a clear decrease of the settling rate, since the slope of the absorbance vs time curve decreases with the concentration of OA. Finally, at OA concentrations higher than 1.57 M, there is not any progressive improvement of the stability.

The decrease of the sedimentation rate as OA concentration increases must be originated by the progressive OA covering of iron particles. As a consequence, the stabilization mechanism must be originated by the progressive structuration of the OA molecules in adsorbed multilayers. This behavior drives steric repulsion among the OA-covered iron particles and, therefore, a decrease of settling rate.

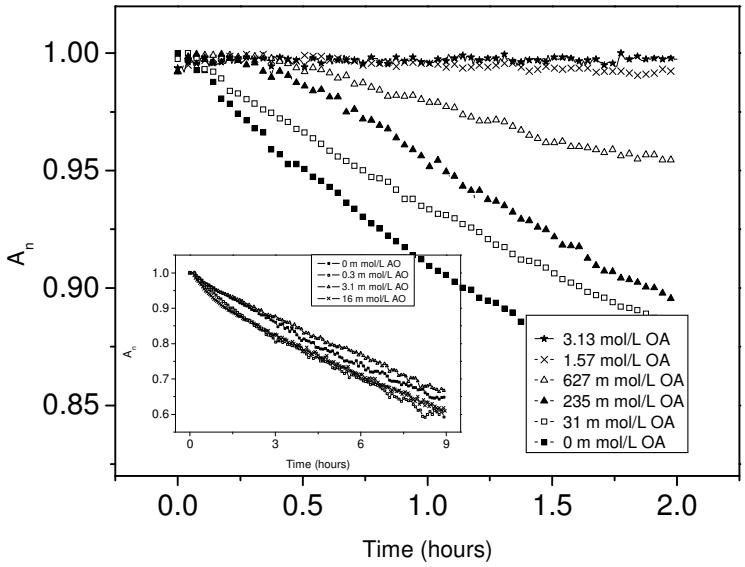

Fig. 3. Normalized absorbance, $A_n = A/A_0$, as a function of time for suspensions containing 0.017 vol% of iron and the indicated OA concentration. (From [22]).

C. Effect of silica nanoparticles. These experiments were carried out for suspensions containing 0.017 vol% of iron and silica nanoparticles concentration up to 24.3 mM. The results of these tests are shown in Figure 4. As can be observed, suspensions with silica concentration below 2.4 mM settle rather quickly. This behavior is a direct consequence of the existence of iron-silica adhesion, which provokes a growing of the particle size and, therefore, a faster settling rate than in the absence of silica. Notice that the existence of heterogeneous aggregation among silica and magnetic particles in similar systems was proved earlier [23, 24]. On the other hand, for silica concentration higher than 2.4 mM the formation of a network of silica particles, by inter-particle hydrogen bonding, that imparts a gel-like structure to the suspension [6, 9], is the dominant phenomenon. For 4.8, 7.3 and 12.2 silica concentration the absorbance increases at the beginning of the experiment and then it falls down. This can be explained considering that, at the beginning, the iron-silica gel scatters the light that otherwise would strike the detector of the spectrophotometer. However, after a time these iron-silica structures break and fall down, since silica concentration is still too low. Finally, as can be seen in Figure 4, for silica concentration of 24.3 mM the iron-silica network is stiff enough to hold in suspension the entire iron load (absorbance remains constant with time).

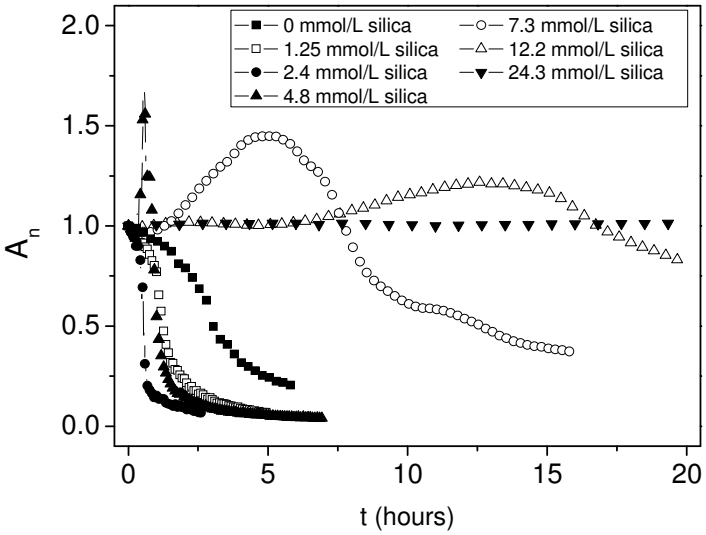

Fig. 4. Normalized absorbance, $A_n = A/A_0$, as a function of time. All suspensions contained 0.017 vol% of iron and the silica concentration indicated. (From [22]).

3.2. Sedimentation Behavior in Concentrated Suspensions

A. Experimental. Iron powder was used as magnetic particles. Kerosene (Sigma-Aldrich, Germany) was used as liquid carrier. Oleic acid (OA), aluminum stearate (AlSt) (technical quality) (Sigma-Aldrich, Germany) and silica nanoparticles were used as stabilizing additives. Iron-OA and iron-AlSt suspensions were prepared as described above for diluted iron-OA suspensions. Iron-silica suspensions were also prepared in the same way described above for diluted suspensions.

The method used for measuring the particle sedimentation rate in magnetorheological fluids is based on the time evolution of the electromotive force induced in a coil that surrounds the sample. A detailed description of the experimental setup as well as details of the fundamentals of the method can be found in [16]. Briefly, the sedimentation behavior of the suspensions was estimated from the time evolution of the dimensionless induced potential Δv.

$$\Delta v \propto \frac{\Phi(t)}{1-\Phi(t)} \tag{3}$$

where $\Phi(t)$ is the instantaneous iron volume fraction in the region surrounded by the sensing coil.

B. Comparison between the stabilization effects of OA and AlSt. In order to compare the stabilization efficiency of OA and AlSt, in Figure 5 are represented Δv vs time for iron and iron/OA or AlSt suspensions. As observed, Δv decreases faster with time the larger the OA or AlSt concentration. This can be explained by considering that, in the absence of OA (or AlSt), aggregation must be present because of van der Waals interaction and magnetic attraction due to the weak remnant magnetization of the iron particles. Presumably, large aggregates are formed that span the walls of the test tube (1 cm in diameter). It is precisely the friction with the walls that must hinder their gravitational settling. When surfactants are added, Δv decreases faster than in their absence, this is in fact an indication of diminished aggregation: individual particles or small aggregates sediment more easily than large flocculi spanning the tube. Similar trends are obtained for OA and AlSt suspensions, although an AlSt concentration approximately seven times higher than that added in iron/OA suspensions is required to produce the same change in the stability properties, indicating that OA is a more efficient surfactant than AlSt concerning the stabilization against irreversible iron aggregation in oil-based MR fluids.

C. Effect of silica nanoparticles. Whereas OA and AlSt are surfactants that avoid iron particle aggregation by means of steric repulsion, silica nanoparticles create a gel-like structure that hinders particles settling. Therefore, it is worth to analyze the effect of silica nanoparticles on the settling behavior of concentrated suspensions and to compare it with that of OA and AlSt. Figure 6, where the dimensionless induced potential Δv is plotted as a function of time, shows clearly that, as expected, the sedimentation rate decreases because the carrier is progressively thickened as the silica concentration increases.

For 83 mM silica concentration the thickening effect is not enough to produce any noticeable improvement on the stability properties. For higher concentrations (up to 167 mM silica) the gel formed significantly reduces the sedimentation rate, but it is not yet sufficiently thick to maintain the iron particles in suspension. Only for a concentration as high as 333 mM, the gel completely avoids particle settling, and Δv is practically constant in the time interval studied.

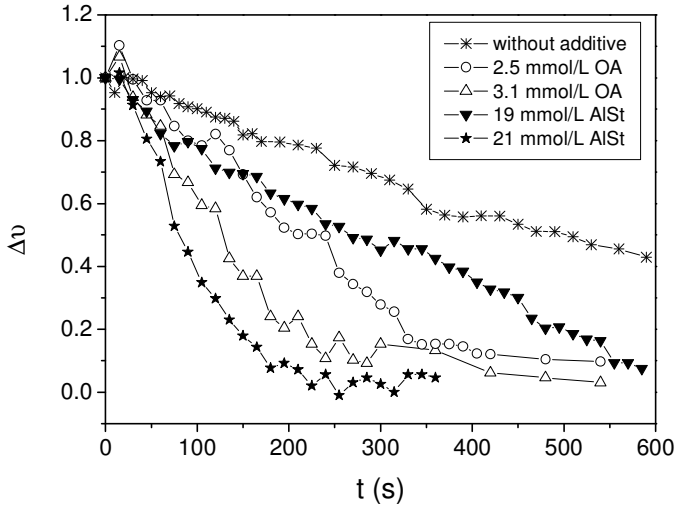

Fig. 5. $\Delta\upsilon$ vs time for suspensions containing 10 % iron volume fraction and the indicated initial concentrations of oleic acid (OA) and aluminum stearate (AlSt).

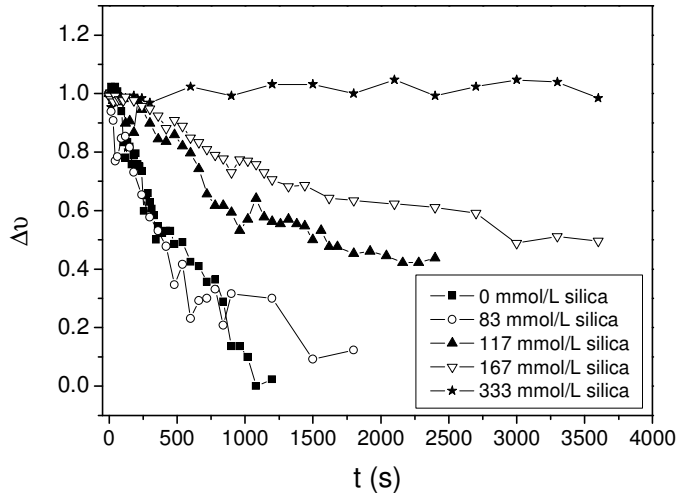

Fig. 6. Dimensionless increment of the induced potential ($\Delta\upsilon$) as a function of time for suspensions containing 10 % iron volume fraction, and the indicated silica concentrations. (From [25]).

4. STABILITY OF MAGNETIC FLUID COMPOSITES

4.1. Preparation of Magnetic Fluid Composites

The magnetic fluid composites (MFC) studied in this paper are composed of micron-sized iron particles (BASF, Germany) dispersed in ferrofluids, prepared as described in paragraph 2, which contain oleate-covered magnetite dispersed in kerosene. To prepare these MFC, proper amounts of iron and ferrofluids were mixed, and the mixtures were shaken and finally immersed in a Branson sonifier. All the suspensions contained the same iron volume fraction $\Phi = 10$ %, while the magnetite volume fraction in the ferrofluids (ϕ) ranged from 0 to 24 %. The sedimentation behavior of these suspensions was studied by the electromagnetic method described earlier.

4.2. Sedimentation Study

Figure 7 shows the sedimentation behavior of iron/magnetite suspensions. Our reference is the curve in the absence of magnetite ($\phi = 0$). First of all, we observe that the addition of a small amount of Fe_3O_4 implies an increase in sedimentation rate (see curves for $\phi = 0.03$ and 0.06), as compared with the suspension of iron in pure kerosene ($\phi = 0$). This fact can be attributed to the irreversible aggregation between iron particles in the absence of Fe_3O_4 nanoparticles, which provokes the formation of big aggregates that spread all over the tube slowing the gravitational settling. When ferrofluid carriers are used, the irreversible aggregation is prevented.

Now, let us consider only the curves corresponding to suspensions containing magnetite. As observed, an increase in magnetite volume fraction implies a decrease in the sedimentation rate that, in principle, could be attributed to the increase in the viscosity of the ferrofluid carriers. In order to check this hypothesis, a new sedimentation experiment was carried out using a $\Phi = 10$ % iron suspension in silicone oil. The result of this experiment is shown in Figure 8. As can be seen, the sedimentation rate in silicone oil ($\eta = 62.3$ mPa·s) is even slightly higher than in the ferrofluid with $\phi = 24\%$ ($\eta = 40.4$ mPa·s).

Therefore, it seems that the progressive stabilization of the suspensions as the magnetite content increases cannot be exclusively ascribed to an increase in the drag force on the settling iron particles. As a consequence, the high stabilization achieved using a ferrofluid as continuous medium, could be associated to some kind of internal structuration of the particles in the suspension. This structure would avoid the aggregation between iron particles, favored by van der Waals and magnetic attractions.

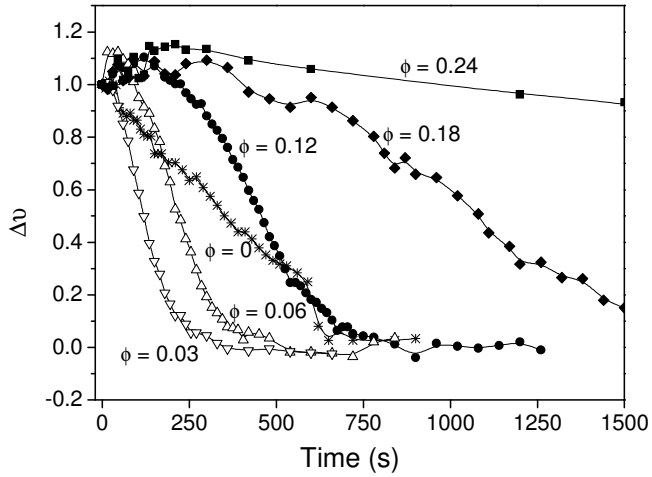

Fig. 7. Dimensionless increment of the induced potential ($\Delta\upsilon$) vs time for iron suspensions (iron volume fraction Φ = 0.1) with different ferrofluid carriers. The magnetite volume fraction of the ferrofluids, ϕ, is indicated. (From [16]).

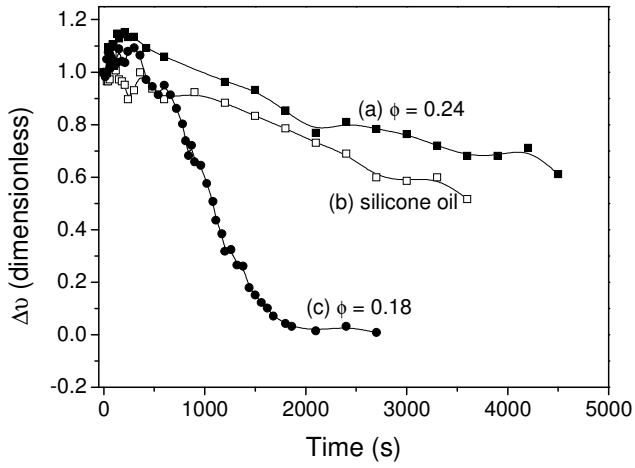

Fig. 8. Similar to Figure 11, using the following carriers: (a) magnetite/kerosene ferrofluid (ϕ = 0.24; η = 40.4 mPa·s), (b) silicone oil (η = 62.3 mPa·s), and (c) magnetite/kerosene ferrofluid (ϕ = 0.18; η = 20.4 mPa·s). (From [16]).

4.3. Electron Microscopy

In order to investigate any possible internal structure of the suspensions, TEM pictures were also taken from particles extracted from diluted (1:1000)

samples. Figure 9a corresponds to particles extracted from a suspension that initially contained 10 vol% of iron. As can be seen, some iron aggregates persist even after diluting the suspension. Figure 9b corresponds to an initial iron (Φ = 10%) - magnetite (ϕ = 24%) suspension. In this case, iron aggregates have disappeared, and a "halo" of magnetite nanoparticles surrounds each particle of iron. This is presumably because of the magnetic attraction between the permanent magnetic moment of the single-domain magnetite particles and the induced magnetic moment of the iron particles.

Summarizing, the use of extremely bimodal iron-magnetite suspensions has been shown to be an efficient way to slow down settling and to prevent irreversible iron aggregation in MR fluids.

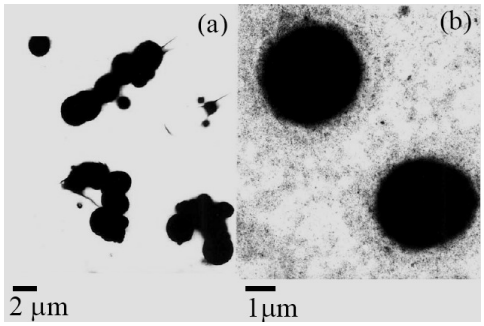

Fig. 9. TEM pictures of diluted suspensions (1:1000 as compared with those used in sedimentation experiments): (a) $\Phi = 0.1$, $\phi = 0$; and (b) $\Phi = 0.1$, $\phi = 0.24$. (From [16]).

5. CONCLUSIONS

It is possible to prepare stable ferrofluids in highly non-polar liquid carriers by chemical co-precipitation of ferric and ferrous ions in the presence of oleic acid. The thermodynamic analysis demonstrated that the loss of stability when the dielectric constant of the carrier liquid is increased is a consequence of the combined action of van der Waals and solvation (lyophobic) forces. The magnetization analysis of the ferrofluids indicates that there exists some degree of particle structuration, induced by both interfacial and magnetic attractions between the particles dispersed in the liquid phase, even in carriers with a very low dielectric constant.

It is feasible to stabilize concentrated iron suspensions against irreversible aggregation processes in oil media by means of the adsorption of fatty acids (oleic acid) or salts (aluminum stearate) on the magnetic particles. The adsorbed molecules impart the needed steric barrier to hinder agglomeration among iron particles.

The addition of silica nanoparticles to stabilize concentrated iron suspensions in oil carriers against aggregation and sedimentation processes is a very efficient mechanism under rest conditions. Unfortunately, under shearing, particle settling is facilitated by the breakage of the silica network and compact sediments, which could make difficult the redispersion, are created.

It is possible to stabilize magnetorheological fluids against aggregation and sedimentation processes by using a ferrofluid as carrier fluid. The magnetic attraction between the nanoparticles (magnetically single-domain) and the micron-sized particles (magnetically multi-domain) favors the formation of clouds of magnetite nanoparticles around each iron one.

Acknowledgments. The authors wish to express their appreciation and deep recognition to the scientific merits and human personality of Prof. Emil Chibowski. He undoubtedly constitutes a role model for young scientists.
Financial support by Ministerio de Educación y Ciencia (Spain) and FEDER funds (EU) under Project No. MAT2005-07746-C02-01, and Junta de Andalucía (Spain) under Project FQM410 are gratefully acknowledged. One of the authors (M.T. López-López) also acknowledges financial support by Secretaría de Estado de Universidades e Investigación (Ministerio de Educación y Ciencia, Spain) through its Postdoctoral Fellowship Program (No. EX2006-0467).

6. REFERENCES

[1] P. P. Phulé, J. M. Ginder, *MRS Bulletin*, 23, 19-21 (1998b).
[2] S. W. Charles, in *Ferrofluids* Odenbach, S. Ed. Springer: Berlin, Germany, Vol. 1, pp 3-18 (2002).
[3] P. P. Phulé, J. M. Ginder, in *Proc. 6th Int. Conference on Electro-rheological Fluids, Magneto-rheological Suspensions and their Applications* Nakano, M. Koyama, K. Ed. World Scientific: Singapore, vol. 1, pp 445-453 (1998a).
[4] S. Odenbach, *Colloid Surface A*, 217, 171-178 (2003).
[5] R. E. Rosensweig, *Sci. Am.*, 247, 136 (1982).
[6] G. Bossis, O. Volkova, S. Lacis, A. Meunier, In *Ferrofluids* Odenbach, S. Ed. Springer: Berlin, Germany, vol. 1, pp 202-230 (2002).
[7] J. M. Ginder, *MRS Bulletin*, 23, 26-29 (1998).
[8] J. M. Ginder, In *Encyclopedia of Applied Physics* Trigg, G. L. Ed. VCH: Weinheim, Germany, vol. 16, pp 487-503 (1996).
[9] O. Volkova, G. Bossis, M. Guyot, V. Bashtovoi, A. Reks, *J. Rheol.*, 44, 91-104 (2000).
[10] Dang, A. Ooi, L. Fales, J. Stroeve, P. *Ind. Eng. Chem. Res.*, 39, 2269-2274 (2000).
[11] G. A. Van Ewijk, G. J. Vroege, A. P. Philipse, *J. Magn. Magn. Mater.*, 201, 31-33 (1999).
[12] Chen, Z. Y. Tang, X. Zhang, G. C. Jin, Y. Ni, W. Zhu, Y. R. In *Proc. 6th Int. Conference on Electro-rheological Fluids, Magneto-rheological Suspensions and their Applications* Nakano, M. Koyama, K. Ed. World Scientific: Singapore, vol. 1, pp 486-493 (1998).
[13] B. D. Chin, J. H. Park, M. H. Kwon, O. O. Park, *Rheol. Acta*, 40, 211-219 (2001).
[14] J. H. Park, B. D. Chin, O. O. Park, *J. Colloid Interf. Sci.*, 240, 349-354 (2001).
[15] P. J. Rankin, J. M. Ginder, D. J. Klingenberg, *Curr. Opin. Colloid In.*, 3, 373-381 (1998).

[16] M. T. López-López, J. de Vicente, G. Bossis, F. González-Caballero, J. D. G. Durán, *J. Mater. Res.*, 20, 874-881 (2005).
[17] M. T. López-López, J. D. G. Durán, A. V. Delgado, F. González-Caballero, *J. Colloid Interf. Sci.*, 291, 144-151 (2005).
[18] C. J. van Oss, *Interfacial Forces in Aqueous Media.* Marcel Dekker, New York, 1994.
[19] R. Massart, *IEEE T. Magn.*, MAG-17, 1247-1248 (1981).
[20] R. Kaiser, G. Miskolczy, *J. Appl. Phys.*, 41, 1064-1072 (1970).
[21] B. D. Cullity, *Introduction to Magnetic Materials,* Addison-Wesley: Reading, Massachusetts, 1974.
[22] M. T. López-López, J. de Vicente, F. González-Caballero, J. D. G. Durán, *Colloid Surface A*, 264, 75-81 (2005).
[23] J. de Vicente, M. T. López-López, F. González-Caballero, J. D. G. Durán, *J. Rheol.*, 47, 1093-1109 (2003).
[24] G. A. Van Ewijk, A. P. Philipse, *Langmuir*, 17, 7204-7209 (2001).
[25] M. T. López-López, A. Zugaldía, F. González-Caballero, J. D. G. Durán, *J. Rheol.*, 50, 543-560 (2006).